

## INVESTIGATION OF OPTICAL RADIATION EXTINCTION BY AEROSOL IN WINTER

V.N. Uzhegov, Yu.A. Pkhalagov, and N.N. Shchelkanov

*Institute of Atmospheric Optics,  
Siberian Branch of the Russian Academy of Sciences, Tomsk  
Received May 18, 1994*

*In this paper we discuss statistical properties of aerosol extinction of visible and IR radiation from field measurements of spectral transmission of the atmosphere along a horizontal path. The measurements have been carried out in winter under three different types of optical weather (haze, ice mist, and snowfall). We also compare in this paper the spectral behavior of the aerosol extinction coefficients measured in Tomsk and near Moscow.*

One of the urgent problems of atmospheric optics is obtaining of statistically supported data on optical characteristics of ground aerosol, in particular, spectral coefficients of aerosol extinction in different climatic regions. The importance of these data is determined, first of all, by ecological and climatic problems as well as different applied aspects related to operation of different optical instrumentation through the atmosphere. The possibility of recording aerosol pollution, its evolution and destruction, establishment of pollution temporal trends, etc., makes it possible to solve a lot of ecological problems. The statistically supported data on aerosol extinction are also needed for taking account of aerosol component in climatic problems.

Most experimental data on aerosol extinction coefficients in the visible and IR ranges obtained in different regions of the former USSR are related to warm seasons.<sup>1-4</sup> The conduction of such experiments in winter presents great engineering difficulties. That is why there is little information about such experiments.<sup>5,6</sup> To make these data more numerous, the 24-hour observations of spectral transmittance of the atmosphere were made near Tomsk from the 3rd to 22nd of December, 1992. The measurements were carried out along the horizontal path with 1-km reflection (the distance to reflecting mirror was 500 m) using an automated multiwave meter of spectral transmittance of the atmosphere.<sup>7</sup> The measurement periodicity was 2 hr. We obtained 199 realizations of spectral coefficients of aerosol extinction ( $\alpha_\lambda$ ) at 22 discrete points of the spectral range between 0.44 and 12.4  $\mu\text{m}$ .

Visual observations of the state of the atmosphere as well as *a posteriori* analysis of spectral behavior of the coefficients  $\alpha_\lambda$  made after preliminary processing of measurement results made it possible to divide the entire data array into four subarrays: snowfall ( $n = 79$  cases), ice mist (35), dense haze (7), and haze (59). It should be noted that the first two types of optical weather were determined visually, whereas the haze and dense haze were determined after preliminary analysis of the experimental data. It should also be noted that the term <ice mist> symbolizes the presence of minor ice crystals formed at temperature lower than  $-12^\circ\text{C}$  and relative

humidity of 70–90% under clear anticyclonic weather.<sup>5</sup> The largest particles of ice mist are well observed in the Sun rays.

Since the air temperature is, according to Ref. 5, a criterion which makes it possible to distinguish between the ice mist and haze, it is interesting to consider the probability of appearance of these two types of optical weather in the given temperature interval as well as at the given absolute and relative air humidity of the atmosphere the observations of which were made simultaneously with measurements of optical characteristics. This information on air temperature ( $t^\circ\text{C}$ ), partial pressure of water vapours ( $e$ , mb), and relative air humidity ( $R$ , %) is given in Table I. As seen from the table, the ice mist is formed in the atmosphere, as a rule, at air temperature  $t < -15^\circ\text{C}$  and relative humidity  $R = 80-100\%$ . These estimates are in good agreement with those from Ref. 5 and make the boundaries of ice crystal formation more precise with respect to air humidity.

Table II lists the results of calculating the statistical characteristics of the  $\alpha_\lambda$  arrays related to three types of optical weather, including mean values of  $\alpha_\lambda$ , rms errors  $\sigma_\alpha$ , elements of autocorrelation matrix  $\rho_{\alpha(0.55), \alpha(\lambda)}$ ,  $\rho_{\lambda(1.06), \alpha(\lambda)}$ , and  $\rho_{\alpha(3.9), \alpha(\lambda)}$  as well as the first three eigenvectors of the autocorrelation matrix  $\phi_k(\lambda)$ . Only mean values of  $\alpha_\lambda$  were calculated for dense haze because of a limited number of cases.

The analysis of the averaged spectral dependences of the coefficients  $\alpha$  for two types of optical weather, which are characterized by presence of <gigantic> particles of hydrosols (snowfall and ice mist) in the atmosphere, reveals that a pronounced decrease of the coefficients  $\alpha$  with the wavelength increase is observed in the visible and IR spectral ranges. In particular, for snowfall this decrease occurs in the wavelength  $\lambda$  range between 0.44 and 0.87  $\mu\text{m}$ . Such spectral dependence of the coefficients  $\alpha_\lambda$  strongly testifies to the fact that snowfalls are observed, as a rule, on the background of a usual atmospheric haze. In the IR range in snowfall the coefficients  $\alpha_\lambda$  tend to increase with the wavelength increase from 1 to 12  $\mu\text{m}$ .

TABLE I. Number of cases of haze and ice mist in the given interval of atmospheric meteorological parameters .

Type of optical weather	Air temperature ( $t^{\circ}\text{C}$ )					
	0 - -5	-5 - -10	-10 - -15	-15 - -20	-20 - -25	-25 - -30
Haze	6	25	11	12	3	2
Ice mist	0	0	2	8	18	7
Relative humidity of air ( $R, \%$ )						
< 80						
81 - 90						
91 - 100						
Haze	1		7		52	
Ice mist	0		11		24	
Partial pressure of water vapors ( $e, \text{mb}$ )						
0 - 2						
2 - 4						
4 - 6						
Haze	19		34		6	
Ice mist	33		2		0	

TABLE II. Statistical characteristics of spectral coefficients of aerosol extinction ( $\alpha_{\lambda}$ ) .

$\lambda,$ $\mu\text{m}$	$\alpha_{\lambda},$ $\text{km}^{-1}$	$\sigma_{\alpha},$ $\text{km}^{-1}$	$\rho_{\alpha(\lambda_k), \alpha(\lambda)}$			$\varphi_1(\lambda)$	$\varphi_2(\lambda)$	$\varphi_3(\lambda)$
			$\lambda_k: 0.55$	1.06	3.9			
1	2	3	4	5	6	7	8	9
Haze								
0.44	0.645	0.452	0.989	0.924	0.511	0.522	- 0.249	- 0.268
0.48	0.531	0.373	0.995	0.927	0.539	0.432	- 0.153	- 0.209
0.55	0.451	0.316	1	0.940	0.584	0.368	- 0.073	- 0.095
0.63	0.413	0.290	0.996	0.949	0.604	0.337	- 0.047	- 0.047
0.69	0.365	0.256	0.990	0.957	0.633	0.298	- 0.012	-0.001
0.87	0.274	0.184	0.951	0.958	0.710	0.209	0.083	0.079
1.06	0.315	0.217	0.940	1	0.649	0.244	0.024	0.493
1.22	0.277	0.196	0.895	0.976	0.686	0.212	0.087	0.650
1.60	0.149	0.121	0.866	0.928	0.837	0.128	0.150	0.224
2.17	0.113	0.093	0.720	0.784	0.944	0.083	0.207	0.109
3.91	0.098	0.087	0.584	0.649	1	0.064	0.251	0.057
4.69	0.114	0.085	0.736	0.787	0.865	0.077	0.156	0.076
8.18	0.081	0.075	0.568	0.654	0.890	0.054	0.189	0.090
8.66	0.110	0.091	0.448	0.470	0.926	0.053	0.307	- 0.095
9.12	0.114	0.099	0.453	0.498	0.940	0.058	0.323	- 0.060
9.55	0.129	0.107	0.430	0.445	0.866	0.059	0.342	- 0.182
10.34	0.085	0.079	0.355	0.352	0.861	0.036	0.264	- 0.128
10.66	0.098	0.083	0.363	0.371	0.873	0.039	0.284	- 0.119
11.21	0.103	0.086	0.399	0.409	0.872	0.044	0.289	- 0.123
11.76	0.083	0.076	0.341	0.343	0.853	0.034	0.268	- 0.087
12.19	0.115	0.094	0.431	0.436	0.851	0.052	0.299	- 0.151
Ice mist								
0.44	0.858	0.417	0.988	0.903	0.760	0.346	- 0.385	- 0.218
0.48	0.742	0.380	0.992	0.914	0.776	0.319	- 0.329	- 0.196
0.55	0.680	0.365	1	0.931	0.816	0.312	- 0.248	- 0.124
0.63	0.659	0.345	0.992	0.931	0.819	0.295	- 0.226	- 0.048
0.69	0.613	0.332	0.988	0.949	0.843	0.287	- 0.182	- 0.033
0.87	0.538	0.278	0.951	0.968	0.872	0.238	- 0.081	0.261
1.06	0.563	0.278	0.931	1	0.909	0.239	- 0.014	0.494
1.22	0.517	0.278	0.877	0.974	0.921	0.232	0.069	0.578
1.60	0.391	0.206	0.872	0.959	0.963	0.174	0.109	0.247
2.17	0.361	0.193	0.826	0.927	0.985	0.160	0.160	0.157
3.91	0.365	0.208	0.816	0.909	1	0.171	0.197	0.055
4.69	0.350	0.195	0.773	0.847	0.957	0.154	0.202	- 0.078
8.18	0.335	0.198	0.791	0.863	0.962	0.159	0.199	- 0.126
8.66	0.372	0.211	0.785	0.858	0.981	0.169	0.235	- 0.085
9.12	0.395	0.219	0.800	0.867	0.982	0.178	0.228	- 0.069
9.55	0.375	0.221	0.760	0.796	0.968	0.174	0.256	- 0.072
10.34	0.329	0.192	0.782	0.838	0.965	0.154	0.220	- 0.161
10.66	0.348	0.201	0.776	0.832	0.964	0.160	0.230	- 0.176
11.21	0.346	0.195	0.751	0.822	0.962	0.152	0.239	- 0.160
11.76	0.316	0.196	0.750	0.819	0.955	0.152	0.239	- 0.141
12.12	0.336	0.196	0.776	0.820	0.948	0.155	0.204	- 0.139

TABLE II continued.

1	2	3	4	5	6	7	8	9
Snowfall								
0.44	1.104	0.598	0.951	0.910	0.825	0.177	-0.456	
0.48	0.933	0.531	0.987	0.872	0.816	0.133	-0.379	
0.55	0.879	0.505	1	0.867	0.821	0.126	-0.370	
0.63	0.853	0.494	0.985	0.853	0.832	0.123	-0.339	
0.69	0.802	0.481	0.973	0.861	0.840	0.121	-0.316	
0.87	0.741	0.489	0.953	0.897	0.875	0.126	-0.269	
1.06	0.946	0.717	0.867	1	0.946	0.198	-0.124	
1.22	0.932	0.714	0.861	0.978	0.911	0.191	-0.203	
1.60	0.805	0.734	0.833	0.963	0.990	0.208	0.048	
2.17	0.816	0.786	0.821	0.956	0.997	0.223	0.100	
3.91	0.849	0.828	0.821	0.946	1	0.235	0.117	
4.69	0.896	0.877	0.814	0.944	0.994	0.248	0.137	
8.18	0.938	0.931	0.814	0.942	0.993	0.264	0.156	
8.66	0.948	0.913	0.816	0.933	0.993	0.259	0.158	
9.12	0.956	0.919	0.822	0.936	0.991	0.261	0.147	
9.55	0.964	0.910	0.840	0.940	0.990	0.259	0.106	
10.34	0.918	0.890	0.829	0.934	0.987	0.255	0.128	
10.66	0.905	0.877	0.833	0.939	0.985	0.249	0.110	
11.21	0.919	0.899	0.835	0.948	0.980	0.255	0.088	
11.76	0.933	0.943	0.838	0.957	0.977	0.268	0.059	
12.19	0.940	0.934	0.827	0.956	0.966	0.264	0.057	

This tendency can be most probably explained by the fact that the receiving system recorded in snowfalls not only direct radiation but also radiation scattered in the forward direction, the role of which grows with the wavelength decrease.<sup>8</sup> Nevertheless, the contribution of this effect in the visible spectral range turns out to be smaller than the extinction on a haze particles. In the ice mist at the wavelength between 0.44 and 1.6 μm the coefficients α decrease with the wavelength increase, and in the range λ > 1.6 μm the coefficients α are practically independent on λ. Such behavior of the dependence α(λ) indicates that the ice crystals in the atmosphere are also formed on the background of haze.

The analysis of the results listed in Table II shows that in snowfall, ice mist, and haze there is strong correlation between the coefficients of aerosol extinction in the visible and IR spectral ranges which is 0.33 for haze, 0.28 for snowfall, and 0.42 for ice mist.

However, in hazes, in contrast to snowfall and ice mist, the correlation is destroyed substantially in the wavelength range λ > 8 μm where the coefficients ρ<sub>α(0.55), α(λ)</sub> are only 0.3–0.4.

The eigenvectors φ<sub>k</sub>(λ) and eigenvalues μ<sub>k</sub> of the autocorrelation matrix ρ<sub>α(λ), α(λ)</sub> in conjunction with other statistical characteristics ᾱ(λ) and σ<sub>α(λ)</sub> are known<sup>9</sup> to form a rational set of vector–matrix parameters for optimal (a minimum number of parameters for given accuracy of reconstruction) description of spectral structure of the aerosol extinction coefficients. The approximation of spectral coefficients α<sub>λ</sub> in this case can be represented as

$$\alpha_{\lambda}^j = \bar{\alpha}_{\lambda} + \sum_{k=1}^m C_k^j \varphi_{k, \lambda}, \tag{1}$$

where m is dimensionality of the autocorrelation matrix (or a number of wavelengths λ), k is the number of the eigenvector φ<sub>k, λ</sub>, j is the number of case, and C<sub>k</sub><sup>j</sup> are the expansion coefficients calculated by the formula

$$C_k^j = \sum_{i=1}^m (\alpha_{\lambda_i}^j - \bar{\alpha}_{\lambda_i}) \varphi_{k, \lambda_i}, \tag{2}$$

where i is the number of wavelength λ. The eigenvalues μ<sub>k</sub> of the correlation matrix determine the variance of the expansion (2) coefficients:

$$\mu_k = \frac{1}{N} \sum_{j=1}^N (C_k^j)^2, \tag{3}$$

where N is the number of cases. The eigenvectors and eigenvalues of autocorrelation matrices were calculated by the Jacobi method.<sup>10</sup> The calculation results of the first vectors φ<sub>k, λ</sub> for three types of optical weather are listed in Table II. Table III gives the data on the value of relative stored variances γ<sub>k</sub> calculated by the formula

$$\gamma_k = \sum_{i=1}^k \mu_i / \sum_{i=1}^m \mu_i, \tag{4}$$

where k and m have the same sense as in Eqs. (1)–(3).

TABLE III. Relative value of stored variance γ<sub>k</sub>.

k	Haze	Ice mist	Snowfall
1	0.888	0.882	0.947
2	0.967	0.970	0.979
3	0.985	0.983	0.987

The analysis of calculation results obtained by formulas (1)–(4) and represented in Tables II and III enables one to note the following peculiarities. The spectral sign–constant variations of the coefficients α<sub>λ</sub> described with the first eigenvector forms 88% of variance for haze and ice mist and nearly 95% for snowfall. The spectral behavior of eigenvectors φ<sub>1</sub>(λ) for all three types of optical weather is similar to the wavelength dependence of the standard deviation σ<sub>α</sub>(λ). The sign–changing variations of α<sub>λ</sub> (one change of sign) the character of which is described by the second eigenvector φ<sub>2</sub>(λ) are 8–9% of variance for haze and ice mist and only 3% for snowfall. The change of sign in the second eigenvector for the three types of optical weather occurs at different wavelengths and apparently depends on the presence of gigantic particles in the atmosphere. In haze, for which the content of such

particles in air is minimum, the sign change in the vector  $\varphi_2(\lambda)$  occurs between the wavelengths 0.69 and 0.84  $\mu\text{m}$ . For snowfall (there present gigantic particles of hydrosols) the second vector changes its sign in the range between 1.25 and 1.6  $\mu\text{m}$ . And under ice mist conditions with gigantic ice crystals (their size is smaller than that of snowflakes) the sign change in the vector  $\varphi_2(\lambda)$  occurs in the intermediate region  $\lambda$  in comparison with haze and snowfall between 1.06 and 1.25  $\mu\text{m}$ . Table II gives for haze and ice mist the third eigenvector which is characterized by two changes of sign. Though it possesses only  $\sim 1\%$  of variance, its stable spectral behavior for these types of optical weather with pronounced maximum at  $\sim 1.25 \mu\text{m}$  can be resulted from variability of medium-dispersed aerosol particles whose variations are not correlated with sub-micron and gigantic particles. The spectral structure of the third eigenvector is not given for snowfall since it possesses less than 1% of variance.

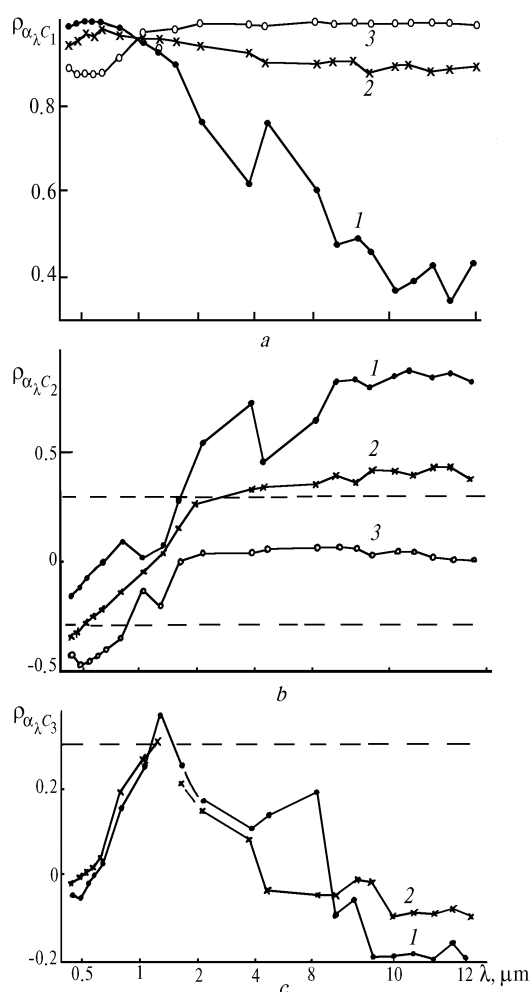


Fig. 1. Spectral dependence of coefficients of correlation between aerosol extinction coefficients  $\alpha_\lambda$  and expansion coefficients  $C_k$  with respect to eigenvectors: first (a), second (b), and third (c) vector. The results correspond to three types of optical weather: haze(1), ice mist(2), and snowfall(3).

In statistical analysis of the measurement results it is of interest to consider the coefficients of correlation between the values  $C_k^j$  and  $\alpha_\lambda^j$ . The results of  $\rho_{\alpha_\lambda, C_1}$  calculations are depicted in Figs. 1 a–c. The dashed lines denote the limits of significance level for the correlation coefficients for 35 cases corresponding to ice mist which are sufficiently close to the remaining types of turbidities.

The analysis of the results depicted in Figs. 1 a–c allows one to note the following peculiarities. Under snowfall the high level of correlation between the values  $\alpha_\lambda$  and  $C_1$  (curve 3, Fig. 1a), particularly in the range  $\lambda \geq 1.6 \mu\text{m}$  ( $\rho_{\alpha_\lambda, C_1} \geq 0.98$ ), indicates that the first eigenvector  $\varphi_{1, \lambda}$  corresponds to variability of precipitation intensity. The second eigenvector  $\varphi_{2, \lambda}$  which is observed in this case only in the visible spectral range caused by the effect of haze particles. Hence, the effect of haze during snowfall is observed not only for mean values of  $\alpha_\lambda$  but on the correlation matrix as well.

In haze strong correlation between the values  $C_1$  and  $\alpha_\lambda$  is observed only in the visible and near IR spectral range (curve 1, Fig. 1) decreasing to the transmission window of 8–12  $\mu\text{m}$  down to 0.3–0.5. This fact reveals that in haze, in contrast to snowfall, the first eigenvector corresponds to variability of finely dispersed aerosol particle fraction. Positive and sufficiently strong correlation between  $\alpha_\lambda$  and  $C_2$  for haze in the IR spectral range (curve 1, in Fig. 1b) can suggest that the second eigenvector in this optical situation can be connected with a coarse-dispersed aerosol particles fraction for which the concentration variations do not correlate with variability of finely dispersed particles of aerosol.

The spectral dependences of coefficient of correlation between  $\alpha_\lambda$  and  $C_1$  and  $C_2$  for ice mist (curves 2, Fig. 1 a and b) occupy an intermediate position between those for haze and snowfall. The form of correlation between  $\alpha_\lambda$  and  $C_1$  enables one to assume that the ice mist by its optical manifestations is close to snowfall.

Figure 1c depicts the spectral dependence of coefficients of correlation between  $\alpha_\lambda$  and  $C_3$  for haze (curve 1) and ice mist (curve 2). In spite of a small contribution of the third eigenvector to the stored variance (Table III), it is seen from Fig. 1c that maximum value  $\rho_{\alpha_\lambda, C_3}$  at wavelength about 1.22  $\mu\text{m}$  exceeds the level of significance of the correlation coefficient (a dashed line in Fig. 1c). The third eigenvector is, apparently, caused by variability of a medium-dispersed aerosol fraction which manifests between 1.06 and 1.22  $\mu\text{m}$  and on the averaged dependences of  $\alpha_\lambda$  for these types of optical weather (Table II).

As noted above, the measurement results of aerosol extinction of optical radiation in winter can be found in Refs. 5 and 6. Based on these measurements which were carried out near Moscow, the semiempirical models of reconstructing a spectral structure of aerosol extinction coefficients in winter were developed.<sup>11</sup> In this connection, it is of interest to compare our results with simulation ones from Ref. 11 for certain types of optical weather.

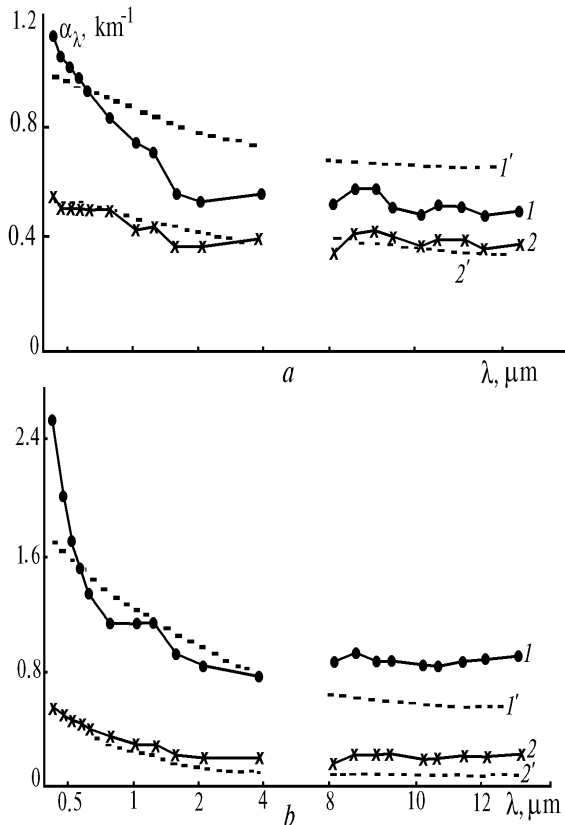


Fig. 2. Comparison between the spectral dependence of averaged aerosol extinction coefficients  $\alpha_\lambda$  obtained in our measurements (1 and 2) and the results of simulating calculations<sup>11</sup> (1' and 2'). Experimental results obtained in ice mist (a) and haze (b) for two values of meteorological visual range.

Fig. 2a depicts the comparison of measured (curves 1 and 2) and calculated (1' and 2') values of  $\alpha_\lambda$  for ice mist. It is seen that the differences between  $\alpha_\lambda$  for light mist ( $S \approx 8$  km) do not exceed 15% (curves 2 and 2') and substantially increase for more thick formations ( $S \approx 4$  km) (curves 1 and 1'). This fact indicates that the suggested model for ice mist<sup>11</sup> can be used only for weak turbidities where contribution of haze component is small. For thicker

mist this model must be refined. Figure 2b represents the spectral dependence of aerosol extinction coefficients in a thick finely dispersed haze formed on the background of ice mist at air temperature  $t < -20^\circ\text{C}$  (curve 1) and in medium-thick haze (curve 2). Since based on classification<sup>11</sup> the curve 1, with respect to the level of turbidity at the wavelength  $\lambda = 0.55 \mu\text{m}$  most close corresponds to mist haze, we compared this curve with the model of mist haze used in this situation with the same visibility results in substantial underestimation of the coefficients  $\alpha_\lambda$  in the spectral ranges  $\lambda < 0.55$  and  $8-12 \mu\text{m}$ . The curve 2' in Fig. 2b corresponds to the model of winter haze near Moscow. Our spectral dependence has a flatter character than that in the model of winter haze near Moscow (curve 2'). The difference between  $\alpha_\lambda$  in the IR spectral range exceeds 100% which indicates that the measurements in Tomsk were made in the presence of more coarse-dispersed haze than that near Moscow.<sup>5,6</sup> The comparison revealed that the available models of aerosol extinction for winter conditions need improvement based on further measurements.

#### REFERENCES

1. M.V. Kabanov, M.V. Panchenko, Yu.A. Pkhalagov, et al., *Optical Properties of Coastal Atmospheric Hazes* (Nauka, Novosibirsk, 1988), 201 pp.
2. V.L. Filippov, A.S. Makarov, and V.P. Ivanov, *Izv. Akad. Nauk SSSR, Fiz. Atmos. Okeana* **15**, No. 3, 257–265 (1979).
3. N.N. Paramonova, A.M. Brounshtein, and V.I. Privalov, *Tr. Gl. Geofiz. Obs.*, No. 496, 84–93 (1985).
4. A.I. Chavro, *Izv. Akad. Nauk SSSR, Fiz. Atmos. Okeana*, No. 3, 270–276 (1985).
5. V.L. Filippov, L.M. Artem'eva, S.O. Mirumyants, *Izv. Akad. Nauk SSSR, Fiz. Atmos. Okeana* **5**, No. 9, 915–920 (1969).
6. V.L. Filippov and S.O. Mirumyants, *Izv. Akad. Nauk SSSR, Fiz. Atmos. Okeana* **1**, No. 7, 818 (1971).
7. Yu. A. Pkhalagov, V.N. Uzhegov, and N.N. Shchelkanov, *Atmos. Oceanic Opt.* **5**, No. 6, 404–408 (1992).
8. M.V. Kabanov and Yu.A. Pkhalagov, *Izv. Akad. Nauk SSSR, Fiz. Atmos. Okeana* **6**, No. 2, 213–217 (1970).
9. A.M. Obukhov, *Izv. Akad. Nauk SSSR, Geofiz.* **1**, No. 3, 432–439 (1960).
10. G. Kramer, *Mathematical Methods of Statistics* [Russian translation] (Mir, Moscow, 1975), 648 pp.
11. V.L. Filippov, A.S. Makarov, and V.P. Ivanov, *Dokl. Akad. Nauk SSSR* **265**, No. 6, 1353–1356 (1982).